ISSN:2321-1156
International Journal of Innovative Research in Technology & Science (IJIRTS)

NUMERICAL SIMULATION OF HYPERSONIC FLOW OVER BLUNT BODIES

A.P. Roychowdhury and C. Unnikrishnan
Aerodynamics R& D Division,
Vikram Sarabhai Space Centre,
Thiruvanthapuram, Pin 695022, Kerala , India.

Abstract

The hypersonic flow over a spherical cap with a cylindrical aft body is simulated numerically using a Compressible Navier-Stokes solver.The simulation has been done for a number of Enthalpy conditions which are obtained by varying the free stream Mach number keeping the free stream pressure and temperature conditions corresponding to an altitude of about 50 KM. The primary objective of the study is to compute the heat flux distribution over the body for these conditions which will be of very high use for re-entry problems. Another important objective of the study is to compare the stagnation point heat flux obtained from the present study with a number of correlations available in the literature. Computational grids are generated for simulations using algebraic techniques. The variation of flow parameters such as the Mach number, Pressure and Temperature obtained from different simulations are presented as palettes. The real gas effect on the simulations with respect to the perfect gas assumption is also clearly presented. Comparisons with experimental data shows that computed stagnation heat fluxes and experimental data closely match each other.

Nomenclature

h	Enthalpy
k	Thermal conductive
Le	Lewis number
M	Mach number
Pr	Prandtl number
P	Pressure
q	Heat flu
R_n	Radius of the spherical body
Re	Reynolds number
U	Vector of conserved variables
ρ	Density
Subscripts :	
w	Wall surface
∞	Reference values
0	Stagnation Condition

Introduction

For Manned Space Programs, the temperature effects of hypersonic flight should be studied in detail for designing the crew module to encounter the severe environmental conditions during the journey through the dense atmosphere. Typically during a planetary re-entry, when a capsule or a space vehicle approaches the relatively dense atmosphere at a very high speed a strong bow shock forms ahead of the vehicle detached from its nose. It is subjected to wide range of pressure, heat transfer and shear levels. They appear as one of the critical points in the design phase of the vehicle mission. Across the shock a large amount of kinetic energy is converted into thermal energy and flows into the body resulting in increasing the body temperature. Proper thermal protection system should be provided to overcome this problem in addition to the consideration of structural loads for which information about the heat flux and pressure distribution over the surface of the body is vital.

A well established method to predict the pressures and heat transfer to the body is the wind tunnel testing where a scaled model of the configuration is exposed to fluid flow in a controlled environment. With major developments in wind tunnel techniques and instrumentation, it is possible to simulate both the Mach number and Reynolds numbers, the two main non-dimensional numbers for the similarity of the flow. But it is still very difficult to simulate the Mach numbers of the order of 30 and so. Even then there can be some limitations on the number of sensors to measure the pressures and heat fluxes. In addition, experimental methods are expensive and time consuming also.

One of the important numerical methods for flow simulations is the computational fluid dynamics popularly known as CFD. It is an integral part of the design process of major aerospace components and CFD is decreasing the dependence on the more expensive, time consuming experimental testing or rather using experimental work effectively and economically. The use of computer based CFD methods will accelerate the design process, reduce preliminary development testing and help create reliable designs of space launch vehicles.

In the present work a compressible viscous finite volume based CFD code UNS2D, described in detail in Ref. [1], is used to simulate the hypersonic flow over a blunt axi-symmetric body at a number of enthalpy conditions. The output from the code, mainly heat flux distribution and pressure distribution is graphically presented. The flow field parameters such as Mach number, pressure and temperature in the flow field is also presented in the form of palettes. The computed stagnation heat flux is compared with a number of correlations available in literature.

For a perfect gas the thermodynamics properties like the specific heat coefficients are assumed to be constant and the transport properties viscosity and thermal conductivity are calculated assuming they are functions of temperature only for which Sutherland formula can be used. This assumption is valid only when the total temperature is below about 2000 K and when the temperatures exceed these values the high temperature gas effects should be considered and an equilibrium air flow computations has to be done. In the present study, the thermodynamics properties are given as a function of density and internal energy and suitable curve fits available in literature [2] are used. Similarly the transport properties are also computed in using suitable curve fits available in literature [3].

In the finite volume method, the computational domain is subdivided into a network of meshes of finite volumes and the governing equations of fluid dynamics are used in integral form. The unknown vector U is required at the centroids of finite volume while the fluxes are required at the cell faces. The flux calculations are done in two stages. The convective part of the flux is evaluated by using up winding scheme for which the Van Leers flux vector splitting method is used. Up winding schemes are numerical techniques for solving the flow equations which will be consistent with the velocity and direction with which information propagates throughout the flow field. To calculate the flux crossing each boundary, the solution vector U is to be evaluated on both sides of the cell surface which can be obtained either by forward or backward extrapolation.

A Monotonic Upstream-Centered Scheme for Conservation Laws (MUSCL) -type approach is employed for the evaluation of the fluxes at the cell interfaces. The Van Albada limiter is used to avoid spurious oscillations of the solution. For calculations of split convective fluxes, the values of the primary variables at the cell face are needed. The cell face values are obtained by forward extrapolation (-) or by backward extrapolation (+). Several types of discretization can be obtained by using different values of κ_1 and κ_2 [Ref. 1] so as to control the degree of up-winding. In the equation [1], φ(R) is the limiter employed which is needed in flows involving shocks. The inviscid convective part of fluxes at the cell interface are according to Van Leer's flux vector scheme.

Boundary Conditions

Proper boundary conditions are to be used for getting the correct realistic solutions. In fact boundary conditions are the critical features driving the solution to the appropriate physical values. The following boundary conditions are used in this problem.

- At solid surface: no-slip boundary condition is employed which means that the velocity on the wall is stationary for a non-moving solid surface. An isothermal wall condition is used specifying the wall temperature as an input.
- At the downstream boundary: The flow variables are interpolated from inside cells if the flow is supersonic. If the flow is subsonic pressure boundary condition is used.
- At the inlet the free stream conditions are imposed.
- At the centre line, the symmetry boundary condition is employed.

Grid Generation

Grid generation is one of the most important and first step in the Computational Fluid Dynamics. This involves mainly discretising the computational domain into a number of meshes or cells in an orderly fashion. Although it looks to be a trivial task for simple bodies, it is really a challenging task when a complex configuration is to be discretised.

One of the simplest methods to generate grids over relatively simple body configurations is the algebraic grid generation technique. The grid can be clustered near any region of interest by using suitable stretching parameters. The clustering of grids is necessary near the solid wall so as to capture the boundary layer properly. Also in regions where high flow gradients due to expansion and shock, the grids need to be clustered so as to capture the flow fields sharply. For the prediction of heat flux and shear stresses the first cell height from the solid walls will have to be in microns. The clustering of grids near the solid body are generated using the following formula

$$h = \frac{s(r - 1.0)}{(r^n - 1.0)}$$

where h is the first cell height, s is the distance, r is the stretching parameter and n is the number of divisions in that distance. The steps involved in the grid generation are:

- Defining the geometry and the coordinate system
- Defining the outer boundary which should be sufficiently away from body and there should not be much change in the flow field

- Choosing the regions of fine or coarse meshing. This includes regions near the solid walls where there will be strong gradients in velocities and temperatures because of boundary layer formation. The fine meshing is also needed in the regions where there is change in geometry.
- The selection of suitable stretching parameter to get the required clustering. As mentioned above a geometrical progression can be used for stretching the grids and the values can be adjusted for getting the required cell heights.

Stagnation Point Heat Flux

The heat transfer near the stagnation point of the nose cone (a blunt body, two-dimensional or axi-symmetric) is of primary importance for the thermal protection design when the body enters into a dense atmosphere with very high velocity. Generally for re-entry blunt bodies, the maximum heat transfer will be at the stagnation point and information about this is very essential. A lot of empirical relations based on experimental studies are available in literature for finding out the stagnation heat flux values. These values can be obtained if the incoming flow conditions are known. In the present study the heat flux values computed numerically is compared with a number of such empirical relations.

One of the early works on stagnation point heating has been made by Fay and Riddell and is still widely in use. The correlation, Ref.[5], is given by

$$q_w = 0.76\ Pr^{-0.6} (\rho_e \mu_e)^{0.4} (\rho_w \mu_w)^{0.1} (du_e/dx)^{0.5} (h_0-h_w) [1 - (Le^{0.52} -1)(h_d/h_0)] \quad (1)$$

In the above two equations the subscript 'e' stands for values outside the boundary layer, 'w' for wall and '0' for stagnation conditions. The term in the square bracket accounts for the contribution of chemical reactions and h_d is the free stream per unit mass dissociation energy. All the quantities in the above equations are in SI units. The term du_e/dx is calculated as

$du_e/dx=R_n^{-1}[2(p_0-p_w)/p_0]^{0.5}$

Another expression given in Ref.[6] for stagnation heat flux is given by

$$q_w=1.83e^{-8}\ R_n^{-0.5}\ \rho_\infty^{0.5}\ V_\infty^{3}\ (1-(h_w/h_0)) \quad (2)$$

with all the quantities radius in m, density in Kg/m^3, velocity in m/s and enthalpy h in J/kg and q_w is in W/cm^2.

Using the numerical results of Navier-Stokes code, De Fillipis [7] got a correlation for stagnation enthalpy h_0 in the range of 2 to 39 MJ/Kg and given by

$$q_w = 90\ (P_0/R_n)^{0.5} (h_0-h_w)^{1.17} \quad (3)$$

where P_0 is the stagnation pressure in atm and R_n is the nose radius body in cm and h enthalpy in MJ/Kg and q_w in W/cm^2.

A somewhat similar expression for the stagnation heat flux, Ref.[8], is the one given by

$$q_w=112.4\ (P_0/R_n)^{0.5}\ (h_0-h_w) \quad (4)$$

where P_0 is the stagnation pressure in atm and R_n is the nose radius body in cm and h enthalpy in MJ/Kg and q_w in W/cm^2.

Another correlation given in Ref.[8], for the stagnation heat flux is

$$q_w = 121.80868\ (P_0/R_n)^{0.5}\ h_0^{1.06696} \quad (5)$$

where P_0 is the stagnation pressure in atm and R_n is the nose radius body in cm and h enthalpy in MJ/Kg and q_w in W/cm^2.

Sagnier and Verant, Ref. [9], has derived a correlation for the stagnation heat flux given by

$$q_w=23.787\ (P_0/R_n)^{0.5}\ [(h_0-h_w)/RT]^{1.069} \quad (6)$$

Where T temperature is 273.15 K and R is the gas constant equal to 288.2 J/Kg K. In the above equation all the units are in SI units.

Another correlation for stagnation heat flux given in Ref.[10] is given by

$$q_w = 11030\ R_n^{-0.5}(\rho_\infty/\rho_{SL})^{0.5}\ (V_\infty/7950)^{3.15} \quad (7)$$

where density in Kg/m^3, velocity in m/s and radius in m and heat flux q_w in W/m^2.

Zuppardi and Espisto [11] has recast the Fay-Riddell formula as follows

$$q_w =(-20.555/h_{0\infty}^{0.8932} + 2.902 \times 10^{-5} h_{0\infty}^{0.1068} - 6.588\times10^{-14} h_{0\infty}^{1.1068})(h_{0\infty}-h_w) \quad (8)$$

where enthalpy is in J/Kg and heat flux in W/m^2.

Results and Discussion

As mentioned earlier, a Navier Stokes code has been used to simulate hypersonic flow over a axi-symmetric spherical cap followed by a cylinder body for different entalpy conditions covering a wide range of Mach numbers from 5 to 30 and entalpies from about 1.5 to 48 MJ/Kg. The free stream conditions corresponds to about 50 km altitude where the presure is about 85 Pascals and Temperature is about 264 K. The radius of the body is taken to be 0.3m and is taken as the reference length. The Reynolds numbers corresponding to these free stream conditions and based on the radius of the sphercial cap are below $2x10^5$ and the flow is assumed to be laminar in the study. The table below shows the freesteam conditions used for simulations.

Table 1: Freesteam conditions used for simulations.

P_∞ = 85 Pa T_∞ = 264 K

Mach Number	Total Enthalpy (h_o) MJ/Kg	Reynolds number
5	1.58	$3.3x10^4$
10	5.55	$6.58x10^4$
14	10.63	$9.21x10^4$
17	15.56	$1.12x10^5$
20	21.43	$1.30x10^5$
22	25.88	$1.45x10^5$
24	30.75	$1.58x10^5$
26	36.04	$1.71x10^5$
28	41.76	$1.84x10^5$
30	47.9	$1.97x10^5$

One of the major requirements in CFD simulation is defining of the initial conditions. If the initial conditions used are closer to the final realistic conditions, faster will be the convergence and can save lot of computer time. In external flow problems the initail solution taken is usually the free stream conditions and in the present study the same technique is used.

Figure 1 shows the computational grid used for the simulation. The grid has got dimensions of 60 points along the body and 80 points normal to the body. The grids are generated using algebraic technques as described above. The height of the first cell from the solid wall is about 10 microns.

One of the important requirement in CFD is the grid independence study which show the sufficiency of the grids used for the simulations. For this purpose, a grid independent study is made with grids increased in both axial and radial directions by about a factor of 1.5. In figure 5 the results obtained with grids 60x80 and 90x120 are shown. It can be seen that the results are very close to each other showing that a grid of 60x80 is sufficient for smulations. For all the Mach numbers the simulations are done with a grid size of 60x80.

Another requirement in CFD is the convergence of the results obtained. Figure 2 show the heat flux distribution for different iterations as shown in the fiures. It can be seen that the results are very well converged as all the three curves are indistingushable from eahc other.

In figures 3,4 and 5 the heat flux and pressure distribution over the body is shown for all the Mach numbers from 5 to 30. The pressure values are given as coefficient of pressure defined in the usual manner with respect to the freestream values. It can be seen from the figures that the heat flux values continuously increase with increse in Mach numbers. In the case of pressure values initially there is a slight increase in pressure coefficient values with increase in Mach nmber, while for higher Mach numbers the pressure coefficient values are almost same with no appreciable changes. In all the figures it can be seen that the heat flux is maximum at the stagnation point and decreases along the body as the flow expands downstream. In the case of pressure also, the behaivour is same with maxmum pressure at the stagnation point and decreases further donwstream because of the flow expansion.

Figures 6, 7 and 8 show the Mach number, pressure and temperature palettes for different freestream Mach numbers as denoted in the figures. The figures clearly show all the features associated with hypersonic flow over these type of bodies. The pressure and temperatures are non dimesnionlaised with respect to the free pressure and temperatures respectively. The detached shock in front of the body, the decrease in Mach number across the shock, the increase in pressure and temperature across shock etc. are all clearly visible from these pictures. It can also be seen that the stand off distance of detached shock decreases with increasing free stream Mach numbers.

As mentioned earlier, at higher Mach numbers the high temperatures real gas effect is to be considered in the simulation for realistic solutions. In figure 9 the differences in heat flux and pressure distribution between perfect and real gas computation for a Mach number of 5 is shown. It can be seen that there is not much difference in both heat flux and pressure distribution over the body and it is expected also as the temperatures involved in the flow is not very high. In figure 10 the heat flux and pressure distribution between perfect and real gas computation is shown for a Mach number of 30. It can be seen that there is an appreciable increase in heat flux near the stagnation point and there is a slight increase in pressure also near the stagnation region. The heat flux is increased by about 20 percent in the case of real gas. In figures 11,12 and 13 the Mach number, pressure and temperature palettes are shown for mach numbers 5 and 30 and for both perfect and real gas computations. In the case of Mach number 5 case, it can be seen that there is not much difference in all the features between perfect and real gas computations. But there is significant difference in the case of Mach number 30 case between perfect and reals gas computations. It can be seen that the pressure across the shock is higher in the case of real gas case and this is reflected in the pressure distribution as shown above. In the case of temperature the differences are very much higher. In the case of perfect gas computation the temperature across the shock is about 180 times the free stream temperature and in the case of real gas it is about 40 times the free stream temperature only. With a free stream temperature of about 264 K, this figures will be about 45000 K for perfect gas and 9900 K for real gas computations. This reflect in the increse in heat flux on the stagnation point as mentioned earlier. It can also be seen that the shock stand of distance is higher for perfect gas and

smaller for real gas as can be seen clearly from the case of Mach 30 computations.

Finally, as mentioned above the knowledge of the value of stagnation heat flux is an important information for the re-entry problems for thermal protection design of the body. A lot of empirical relations based on experimental and theoretical considerations are given above. The computed stagnation heat flux using the code is compared with the values obtained with the various correlations. In Table 2 the computed values and values obtained from the correlations are shown. In figure 14 the stagnation heat flux value is shown against the total enthalpy of the flow and in figure 15 the heat flux value is shown for various Mach numbers. It can be seen that for low Enthalpy or Mach numbers, the values of all the correlations give same values and is in very good match with computed values. For higher enhalpy values there are differences in different correlation values and the present computations give values some what a middle value among the different correlation values. Except the values using equations (2) and (4) other values are in a good match with the computed values and the differences between the computed values and the correlation values are about ± 15 percent which is a very good match considering the complexities involved in measuring and computing the heat flux values. The CFD simulations are compared with four experimental data viz. Rose and Stankevice, Rose and Stark, Horton and Yee. These data are taken from Ref [11]. These are given in Figure 16. They show a reasonable match with CFD computations.

Table 2: Stagnation heat flux (W/cm^2) - CFD & empirical correlation values

M	h_0 MJ/ Kg	CFD	Eqn. 1	Eqn. 2	Eqn. 3	Eqn. 4	Eqn. 5	Eqn. 6	Eqn. 7	Eqn. 8
30	47.9	1364.3	1200.0	1034.6	1526.7	988.7	1397.1	1307.6	1163.6	1479.1
28	41.76	1068.1	979.0	840.4	1203.2	797.7	1118.0	1045.0	936.3	1191.8
26	36.04	857.0	788.0	672.1	932.3	633.9	880.7	821.9	741.4	943.1
24	30.75	691.9	625.0	527.8	724.7	506.4	697.1	649.4	576.2	749.8
22	25.88	525.7	487.0	405.8	542.6	390.5	532.4	494.8	438.0	570.4
20	21.43	403.5	371.8	304.2	393.5	292.5	397.8	365.8	324.4	460.8
17	15.56	234.2	237.2	185.8	227.9	179.1	237.9	219.0	194.4	249.2
14	10.63	123.8	141.5	102.8	118.9	99.8	130.4	118.8	105.5	131.9
10	5.55	41.8	47.0	36.5	38.6	36.3	46.7	41.3	36.5	42.4
5	1.58	4.43	4.1	3.9	3.7	4.4	6.1	4.6	4.1	2.9

Conclusion

The axi-symmetric hypersonic flow over a spherical cap cylinder body is simulated using a compressible Navier- Stokes Solver. Simulations have been done for a number of Mach numbers keeping the free stream pressure and temperature constant. By varying the Mach number from 5 to 30, the incoming flow velocity is changed giving different enthalpies ranging from about 1.5 MJ/Kg to about 48 MJ/Kg. The high temperature real gas effect is considered by simulating the equilibrium flow conditions. The heat flux and pressure distribution over the body is obtained for different simulations and are graphically presented. The Mach number, pressure and temperature palettes shown give the qualitative flow features clearly. The difference between perfect gas and real gas effects are shown graphically. The stagnation heat flux, an important parameter for thermal protection design of the body, is computed with different correlations and compared with the numerically computed values and experimental data.

References

1. Unnikrishnan, C. and Balu, R. "Development of an Unsteady Navier-Stokes Solver for Aerospace Applications: Phase I Two-dimensional/axi-symetric flows", Rept No. VSSC:TR:355:95, 1995

2. Srinivasan, J. , Tannehill, J.C., and Weilmuenster, K.J., "Simplified Curve fits for the Thermodynamic Properties of Equilibrium Air", NASA RP-1181, 1987

3. Srinivasan, S. and Tannehill, J.C., "Simplifies Curve Fits for the Transport Properties of Equilibrium Air", NASA Grant NAGI-313, 1987

4. Baldwin, B.L and Lomax, H. "Thin Approximation and Algebraic model for Separated turbulent flows," AIAA Paper No. 78-257, 1978

5. Fay, J.A. and Riddell, F.R., "Theory of stagnation point heat transfer in dissociated air", Journal of Aeronautical Sciences, Vol. 25 p73 1958

6. Whittington, K.T., "A tool to extrapolate thermal re-entry Atmosphere parameters along a body in trajectory space", M.S. Thesis, Raleigh, North Carolina, 2011

7. De Filippis, F. and Serpico, M. " Air high enthalpy stagnation point heat flux calculation", Jl. of Thermophysics and Heat Transfer, Vol. 124, p608, 1998

8. Purpura, C., De Filippis, F., Trifoni,E., Barrera,P and De Gaetano,G., " Comparison between Probe Stagnation point heat flux Measurements and Correlations Formulas in SCIROCCO Plasma Wind tunnel Tests", 18th AIAA International Space Planes and Hypersonic Systems and Technologies Conference, September 24-28, Tours France, 2012

9. Sagnier, P. and Verant, J.-L., "On the Validation of high enthalpy wind tunnel simulations", Aerospace Science and Technology, Vol 2, n7, p425, 1998

10. Hirschel, E.H., "Basics of Aerothermodynamics", Springer, p34, 2008

11. Zuppardi, G. and Esposito, A. "Recasting the Fay-Riddell formulae for computing Stagnation point Heat Flux", Proc Instn Mech Engrs Vol. 214 Part G p115, 2000

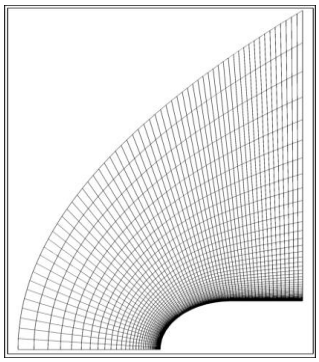

Figure 1: Computational grid over the sphere-cylinder body

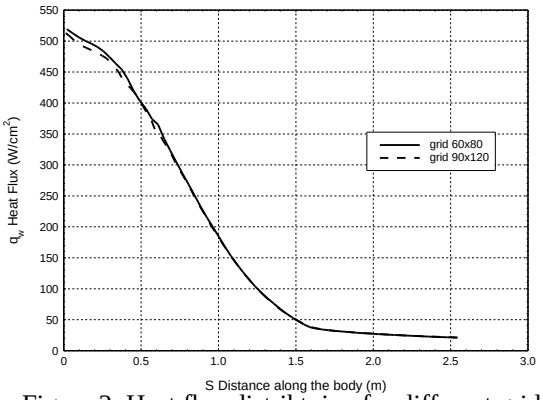

Figure 2: Heat flux distribtuion for different grids

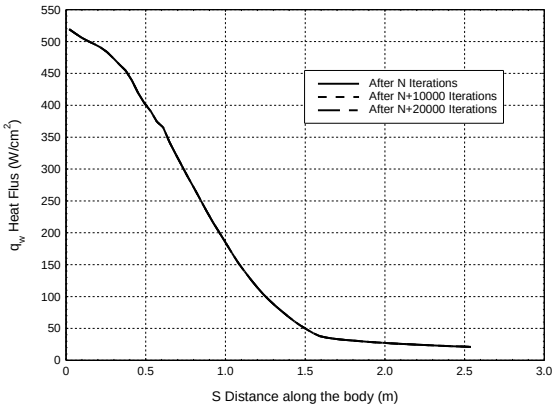

Figure 3: Convergence of heat flux distribtuion

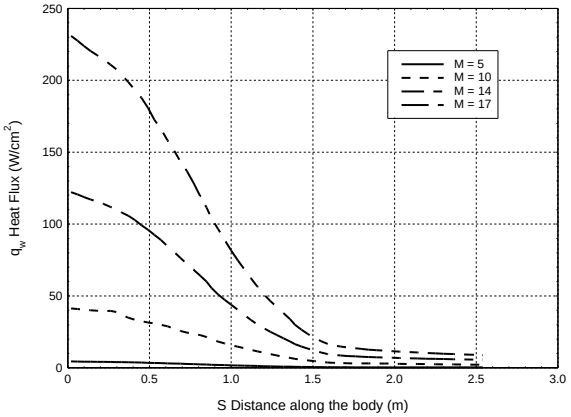

Figure 4a: Heat flux distribution at M=5-17

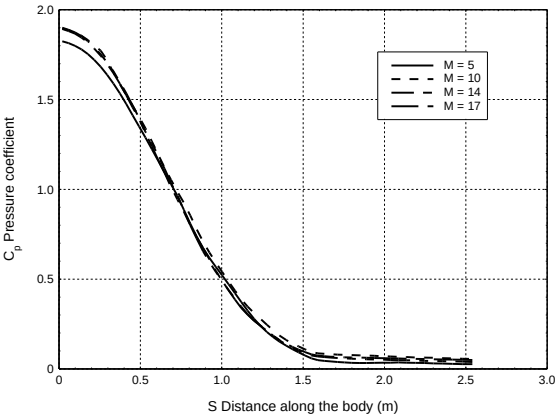

Figure 4b: Pressure distribution at M=5-17

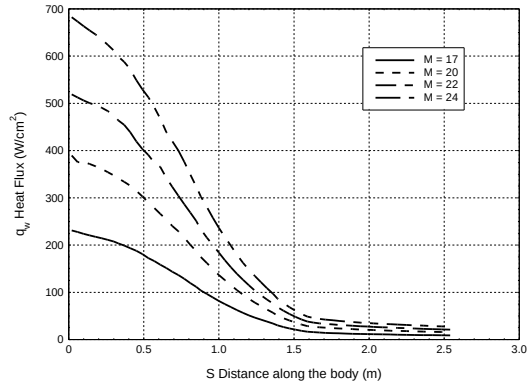

Figure 5a: Heat flux distribution at M=17-24

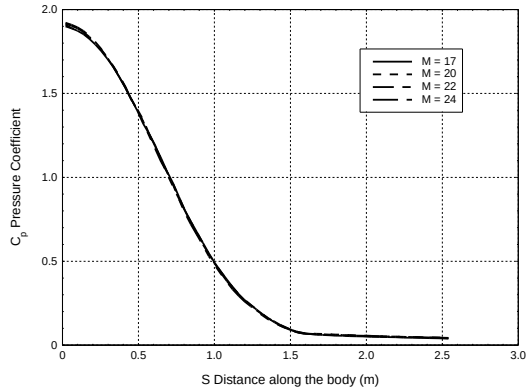

Figure 5b: Pressure distribution at M=17-24

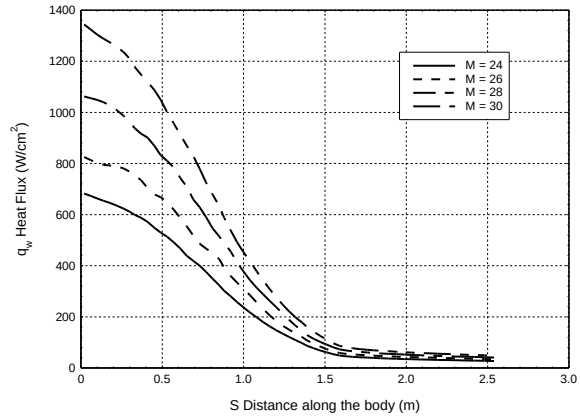

Figure 6a: Heat flux distribution at M=24-30

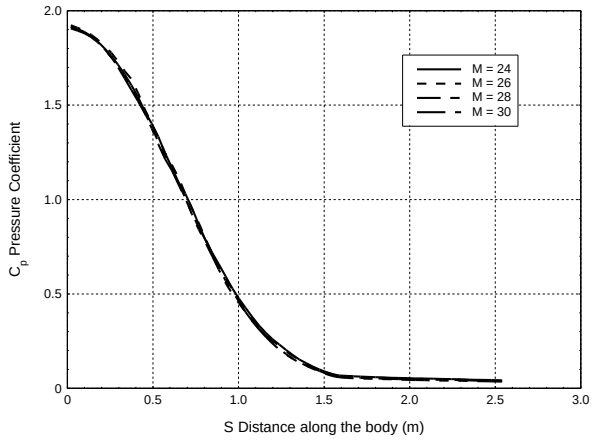

Figure 6b: Pressure distribution at M=24-30

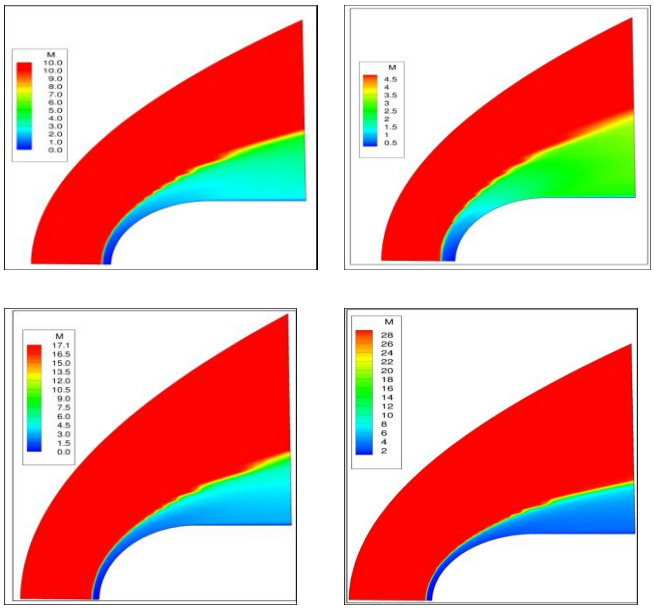

Mach 17 Mach 30

Figure 7: Mach Number Palettes

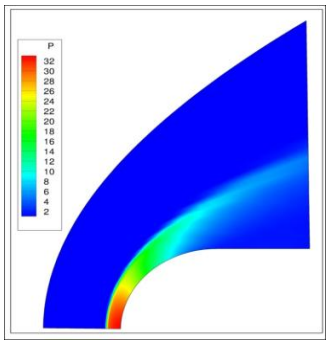
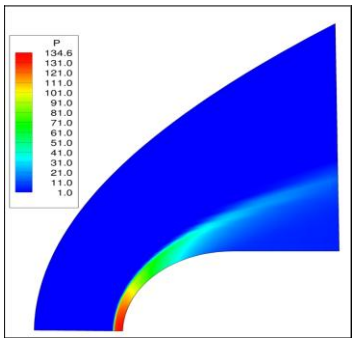

Mach 5 Mach 10

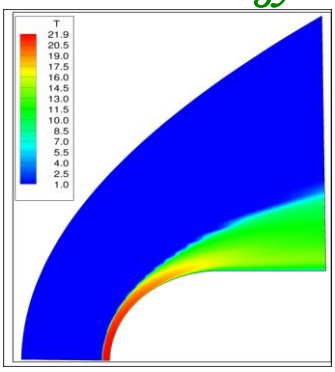
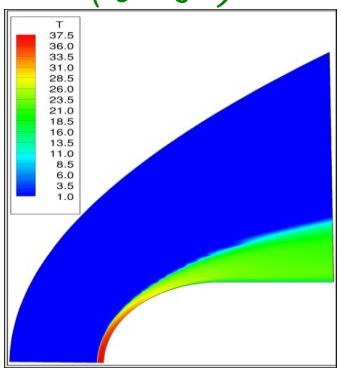

Mach 17 Mach 30

Figure 9: Temperature Palettes

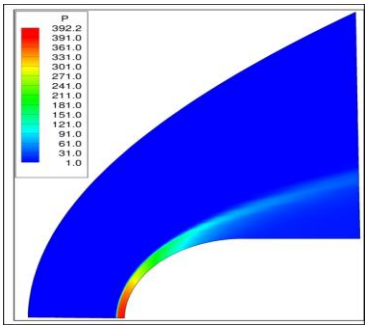
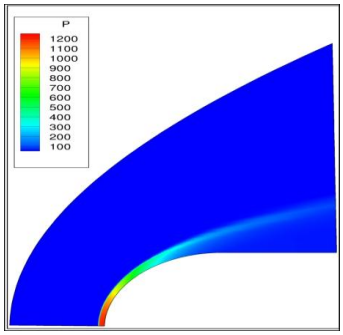

Mach 17 Mach 30

Figure 8: Pressure Palettes

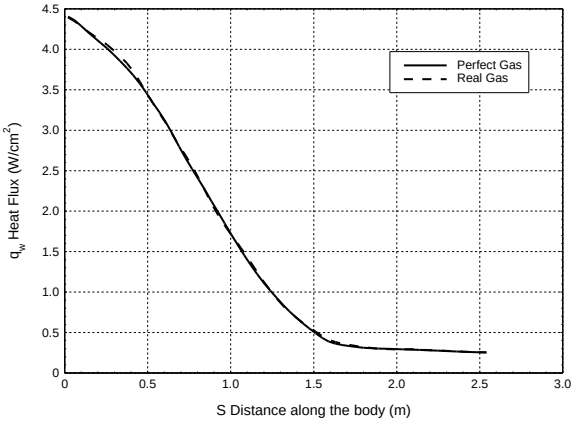

Figure 10a: Heat flux distribution with real and perfect gas at M=5

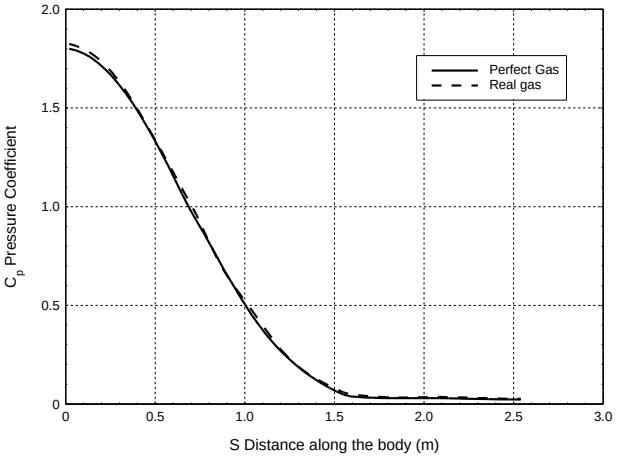

Figure 10b: Pressure distribution with real and perfect gas at M=5

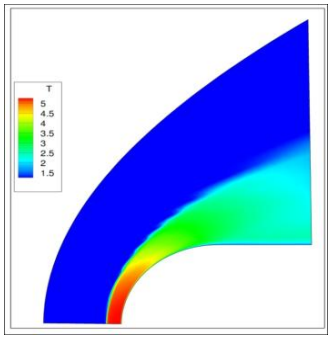
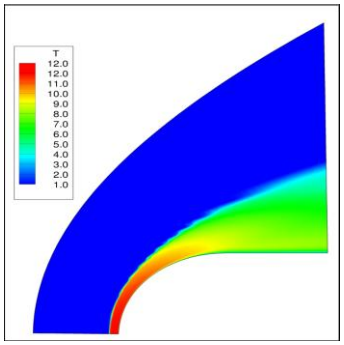

Mach 5 Mach 10

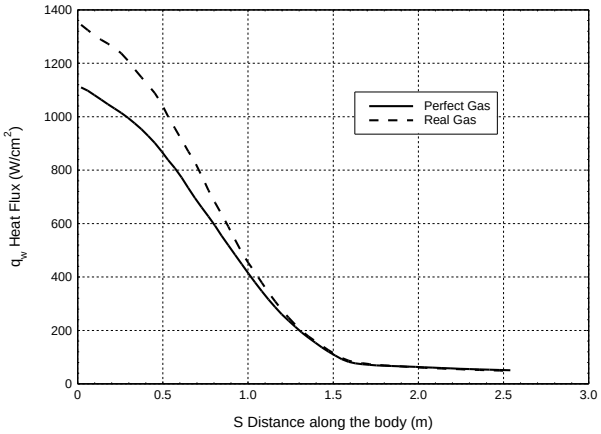

Figure 11a: Heat flux distribution with real and perfect gas at M=30

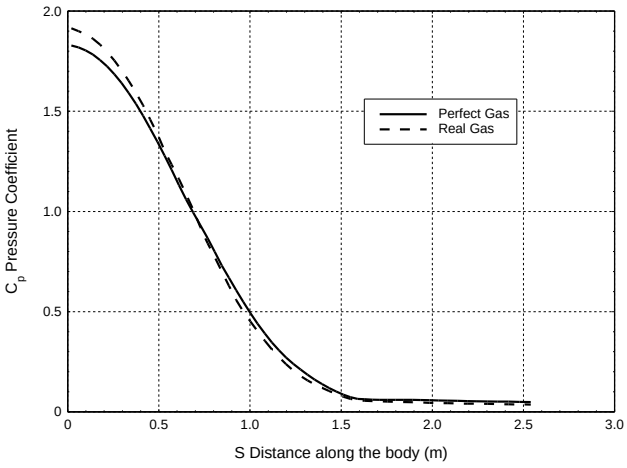

Figure 11b: Pressure distribution with real and perfect gas at M=30

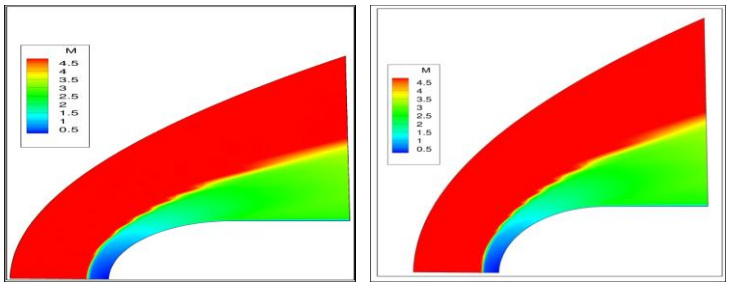

Mach 5 Perfect Gas Mach 5 Real Gas

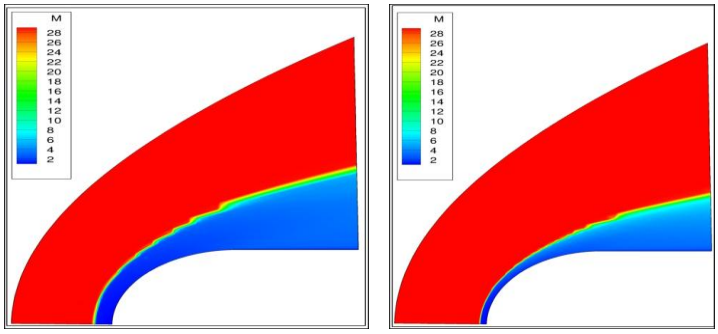

Mach 30 Perfect Gas Mach 30 Real Gas

Figure 12: Mach palettes for perfect and real gases

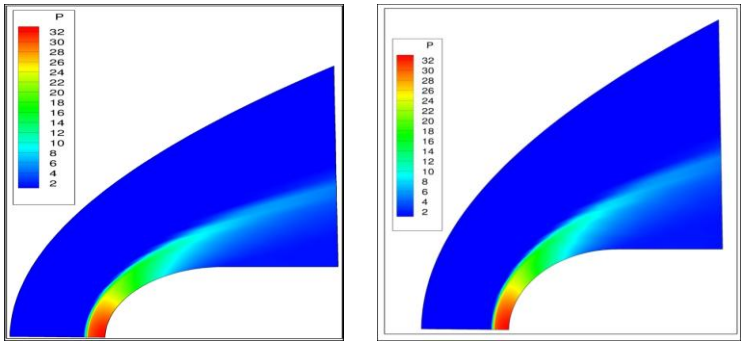

Mach 5 Perfect Gas Mach 5 Real Gas

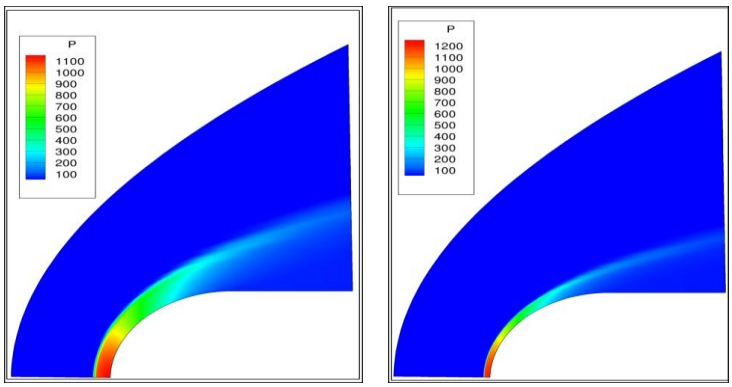

Mach 30 Perfect Gas Mach 30 Real Gas

Figure 13: Pressure palettes for perfect and real gases

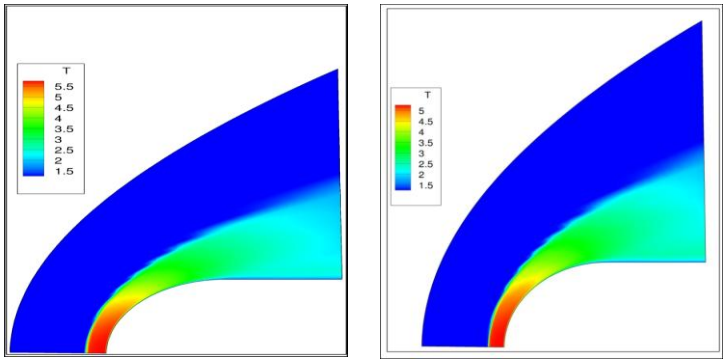

Mach 5 Perfect Gas Mach 5 Real Gas

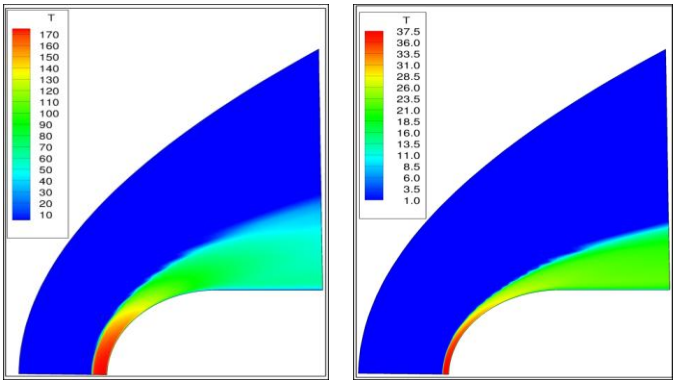

Mach 30 Perfect Gas Mach 30 Real Gas

Figure 14: Temperature palettes for perfect and real gases

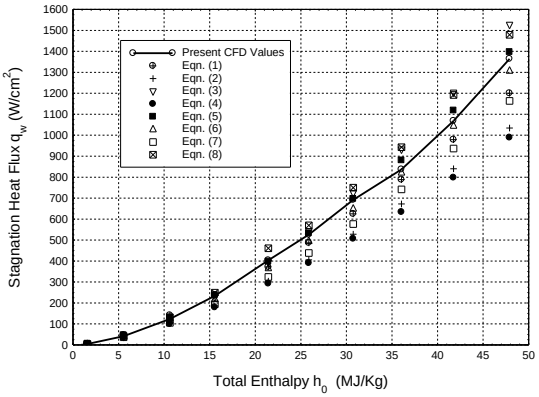

Figure 15: Variation of stagnation heat flux with total enthalpy.

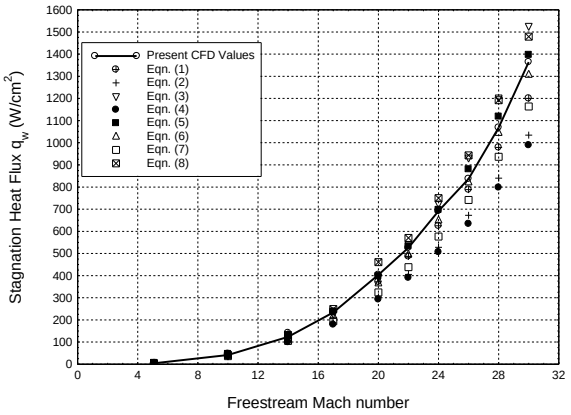

Figure 16: Variation of stagnation heat flux with Mach number

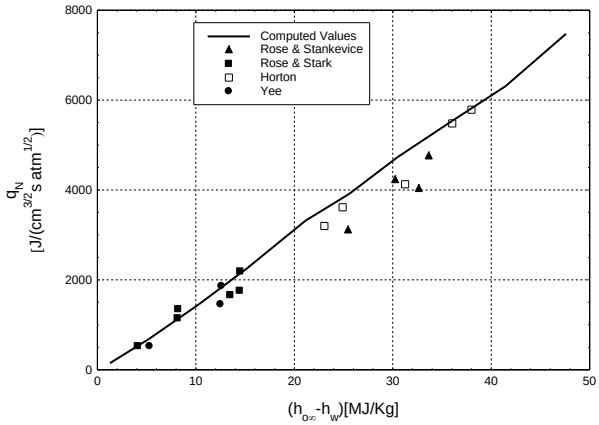

Figure 17: Comparison of CFD values with experimental data